11-30-1988

State Mixing and Vibrational Predissociation in Large Molecule Van Der Waals Complexes: Trans-Stilbene–X Complexes Where X=He, H2, Ne, and Ar

David O. De Haan
University of San Diego, ddehaan@sandiego.edu

Alicia L. Holton
Calvin College

Timothy S. Zwier
Calvin College

State Mixing and Vibrational Predissociation in Large Molecule Van Der Waals Complexes: Trans-Stilbene–X Complexes Where X=He, H2, Ne, and Ar

Abstract

We report a detailed study of vibrational predissociation and intramolecular–intermolecular state mixing in the first excited singlet state of *t r a n s*-stilbene van der Waals complexes with helium, hydrogen, neon, and argon. We present evidence that the helium atom in stilbene–He and the H_2 molecule in stilbene–H_2 possess very low frequency van der Waals bending levels involving delocalization of the complexed species over both phenyl rings. In stilbene–He, the mode-selective, strong coupling of the out-of-plane phenyl ring modes with the pseudotranslation van der Waals modes leads to a dramatic, inhomogeneous broadening of the transitions to several times their breadth in in-plane vibrations. The observed dispersed fluorescence spectra give product state distributions and internal clock lifetime estimates which can only be made consistent with direct lifetime measurements by assuming extensive state mixing of the intramolecular levels with the van der Waals levels in which the states accessed by the laser are actually only about 30% intramolecular in character. We conclude that in these complexes the processes of intramolecular–intermolecular state mixing (static IVR) and vibrational predissociation are not independent processes but are closely tied to one another. In fact, the vibrational product state distributions observed for the out-of-plane phenyl ring levels can best be interpreted as reflecting the percentage van der Waals character in the initially prepared state. In stilbene–H_2 the mode selective coupling exhibits itself as a splitting of the out-of-plane transitions into a set of 5–6 closely spaced transitions separated by only about 1 cm^{-1}. The sequence of transitions is suggestive of an in-plane potential for H_2 motion which is nearly flat across the entire length of the stilbene molecule with a small barrier presented by the ethylenic carbons through which the H_2 molecule can tunnel. Dispersed fluorescence spectra from these levels point to a two-tiered coupling scheme with the bound van der Waals levels. In contrast, the out-of-plane phenyl transitions in stilbene–Ne and stilbene–Ar possess unusual shifts, but the transitions are narrow once again. In these cases the complexed atom appears to be largely localized over a single phenyl ring.

State mixing and vibrational predissociation in large molecule van der Waals complexes: *trans*-stilbene–X complexes where X = He, H_2, Ne, and Ar

David O. DeHaan, Alicia L. Holton, and Timothy S. Zwier[a)]
Department of Chemistry, Calvin College, Grand Rapids, Michigan 49506

(Received 10 August 1988; accepted 30 November 1988)

We report a detailed study of vibrational predissociation and intramolecular–intermolecular state mixing in the first excited singlet state of *trans*-stilbene van der Waals complexes with helium, hydrogen, neon, and argon. We present evidence that the helium atom in stilbene–He and the H_2 molecule in stilbene–H_2 possess very low frequency van der Waals bending levels involving delocalization of the complexed species over both phenyl rings. In stilbene–He, the mode-selective, strong coupling of the out-of-plane phenyl ring modes with the pseudotranslation van der Waals modes leads to a dramatic, inhomogeneous broadening of the transitions to several times their breadth in in-plane vibrations. The observed dispersed fluorescence spectra give product state distributions and internal clock lifetime estimates which can only be made consistent with direct lifetime measurements by assuming extensive state mixing of the intramolecular levels with the van der Waals levels in which the states accessed by the laser are actually only about 30% intramolecular in character. We conclude that in these complexes the processes of intramolecular–intermolecular state mixing (static IVR) and vibrational predissociation are not independent processes but are closely tied to one another. In fact, the vibrational product state distributions observed for the out-of-plane phenyl ring levels can best be interpreted as reflecting the percentage van der Waals character in the initially prepared state. In stilbene–H_2 the mode selective coupling exhibits itself as a splitting of the out-of-plane transitions into a set of 5–6 closely spaced transitions separated by only about 1 cm^{-1}. The sequence of transitions is suggestive of an in-plane potential for H_2 motion which is nearly flat across the entire length of the stilbene molecule with a small barrier presented by the ethylenic carbons through which the H_2 molecule can tunnel. Dispersed fluorescence spectra from these levels point to a two-tiered coupling scheme with the bound van der Waals levels. In contrast, the out-of-plane phenyl transitions in stilbene–Ne and stilbene–Ar possess unusual shifts, but the transitions are narrow once again. In these cases the complexed atom appears to be largely localized over a single phenyl ring.

I. INTRODUCTION

The field of gas-phase van der Waals cluster spectroscopy has had as one of its recent focuses a better understanding of the time scale and mechanism of intramolecular vibrational redistribution (IVR) and vibrational predissociation (VP) of the cluster. A great stimulus to the current intense activity in the field was provided by the work of Janda and co-workers who observed very broad line shapes in the infrared spectra of ethylene clusters.[1,2] Since then, many studies, most of them in the infrared, have focused on determining the energy and mode dependence of the observed linewidths, and the dependence of the linewidth on the nature of the parent molecules involved in the cluster.[2–9] One common feature of most of the studies involving ground state vibrational excitation in the complex is that the laser deposits energy far in excess of the van der Waals binding. Thus, all vibrational modes pumped have vibrational predissociation open to the complexes. Surprisingly, such studies have found large differences in the linewidths of transitions within a single complex, pointing to high mode selectivity in the lifetime-broadening processes. It is sometimes difficult to experimentally determine which process one should associate with the observed linewidths—vibrational predissociation or intramolecular vibrational redistribution of the complex.[10] Growing evidence points to vibrational predissociation as the source of the line broadening observed in the high resolution infrared spectra of most small binary and ternary molecular complexes. In many cases, IVR (probably better referred to as state mixing) is also seen as a localized, *J*-dependent perturbation in the spectrum which reflects the interaction of the intramolecular levels excited by the laser with a sparse set of background levels. Yet it sill remains to be determined how large a role IVR plays in the observed linewidths as the molecules which make up the clusters increase in size.[10]

Several studies utilizing electronic excitation in the complex have addressed similar processes in electronically excited states.[11–14] In favorable cases, studies involving electronic excitation can probe the fate of the intramolecular vibronic excitation by dispersing the fluorescence to determine the fraction of the emission due to resonance fluorescence, IVR, and vibrational predissociation. Of particular interest here is the recent careful work of Butz *et al*[11,12] on the *p*-difluorobenzene–Ar complex. They report striking mode selectivity both in the vibrational predissociation rates and in the vibrational state distributions of the dissociated

[a)] Author to whom correspondence should be addressed. Present address: Department of Chemistry, Purdue University, West Lafayette, Indiana 47907.

 0021-9606/89/083952-15$02.10

products. The authors recognize the possibility that Fermi resonance between the intramolecular vibrational levels and near-isoenergetic combination levels involving large amounts of van der Waals stretching and bending excitation could account for the product state distributions they observe. However, their most recent evidence[12] suggests that such state mixing is not very important in this complex and the authors are left without a clear explanation of their observed product state distributions. Thus, much more needs to be learned about the kinds of complexes, vibrational motions, state densities, and coupling strengths for which state mixing is important. Furthermore, the effect of such mixing on vibrational predissociation needs further clarification. It is on these questions that the body of this work will focus.

We report here a detailed study of the first excited singlet state of several *trans*-stilbene van der Waals complexes. These complexes, by virtue of the low frequency out-of-plane vibrations of the phenyl rings, possess a fine grid of initial energies which in many cases range below the threshold for vibrational predissociation. By choosing a chromophore of this sort we are afforded the opportunity of probing levels ranging from below the predissociation threshold to well above it. We will see that the nature of the vibrational mode excited has a dramatic effect on the appearance of both the fluorescence excitation and dispersed fluorescence spectra of these complexes.

We have previously made a preliminary report[15] of mode-selective broadening in several low-frequency transitions of the first-excited singlet state of *trans*-stilbene van der Waals complexes. In this paper we present a full account of our work which has been extended in several significant ways. First, our recent analysis[16] of the low energy region of the *trans*-stilbene S_1–S_0 spectrum has provided an unambiguous assignment for the low-frequency transitions exhibiting mode selectivity. Second, much of the earlier work was carried out using resonance-enhanced two-photon ionization with total ion collection and thus was restricted to excitation scans. The present results utilize total fluorescence excitation, dispersed fluorescence, and wavelength-resolved fluorescence excitation techniques. The dispersed fluorescence spectra have provided a wealth of new data on the fate of the excitation energy in the complex. The wavelength-resolved fluorescence excitation scans have provided true band shapes of the broadened contours of the stilbene–He complex. The improved signal-to-noise ratio of the fluorescence excitation experiments has allowed us to identify and characterize van der Waals transitions associated with the out-of-plane stilbene vibrations for several other stilbene–X complexes which have in turn shed considerable light on the source of the broadening in these complexes.

II. EXPERIMENTAL

The experimental apparatus has been described previously.[16] For the present experiments the *trans*-stilbene sample was heated to ~110 °C, entrained in buffer gas, and expanded through a pulsed valve. Spectra of the parent compound were recorded with backing pressures of 2–3 atm helium (1 atm = 101.325 kPa). Stilbene–He van der Waals complex transitions were observed at 10–30 atm backing pressure with the valve operating at a minimum open time of about 150 μs. The stilbene–H_2 complex was observed with best intensity when expanding a 2% H_2 in helium mixture through the nozzle at backing pressures of 8–12 atm. Stilbene–Ne complexes were formed from a 5%–10% neon in helium mixture while stilbene–Ar complexes were prepared by using a 1% Ar in helium mixture. Both neon and argon complexes utilized a 5 atm backing pressure. The stilbene–Ar and stilbene–H_2 complex transition intensities were especially sensitive to higher argon or hygrogen concentrations which readily led to broad backgrounds due to higher complex formation.

The jet was crossed 1 cm downstream with the doubled output of an excimer-pumped dye laser (~0.30 cm^{-1} bandwidth in the ultraviolet) which was attenuated to 1 μJ/pulse or less to avoid saturation of the transition when such saturation is a concern. Total fluorescence was detected with an EMI 9829QB photomultiplier tube using gated integration. Dispersed fluorescence spectra were recorded with a 3/4 meter SPEX monochromator at a bandwidth of 6–9 cm^{-1} FWHM.

III. RESULTS AND INTERPRETATION

At the time of our preliminary report[15] on mode-selective broadening in van der Waals complexes of *trans*-stilbene, the low frequency parent transitions which carried the broadened van der Waals transitions had not been assigned. Since then, the partial assignment of Suzuki *et al.*[17] and its extension to a complete assignment by our group[16] have now clearly identified these transitions. An overview of the first 200 cm^{-1} of the $S_1 \leftarrow S_0$ transition taken under high helium backing pressures is shown in Fig. 1. The calculations of Warshel[18] point out two low-frequency transitions of a_u symmetry in C_{2h}: ν_{36} (ethylenic carbon–phenyl out-of-plane bend) and ν_{37} (ethylenic carbon–phenyl out-of-plane torsion). These modes are present in the spectrum only as even overtones and combinations. In addition, there is a strong progression in ν_{25}, an a_g symmetry ethylenic carbon–phenyl

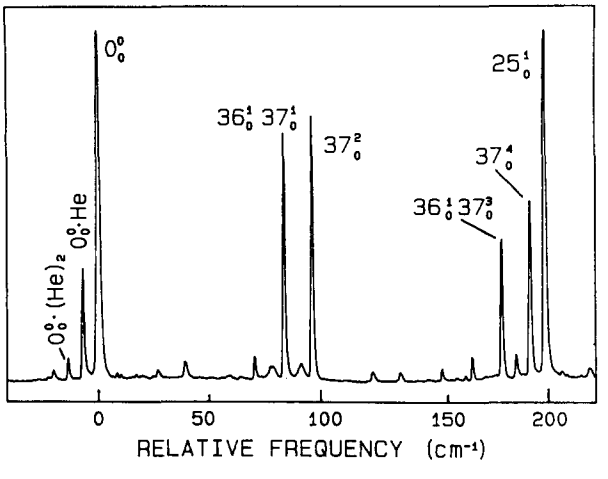

FIG. 1. Partially saturated laser-induced fluorescence excitation spectrum of *trans*-stilbene in the region near the $S_1 < S_0$ origin under expansion conditions (P_0 = 20 atm helium) in which stilbene–$(He)_n$ complexes are present.

in-plane bending mode at 197 cm^{-1}. The entire low-frequency region of the *trans*-stilbene spectrum can be assigned using only these three modes. In particular, the 82 cm^{-1} transition is $36_0^1 37_0^1$ while the 95 cm^{-1} transition is 37_0^2, as is marked in Fig. 1. Much of the remainder of our discussion will concentrate on the van der Waals transitions associated with these parent transitions.

A. Stilbene–He

1. 0_0^0 and in-plane vibrations

The spectrum of Fig. 1 shows the low-energy region near the origin of the $S_1 \leftarrow S_0$ transition under partially saturated laser power conditions. A high backing pressure of helium (15 atm) enables the formation of a series of *trans*-stilbene–He_n van der Waals complexes. The origin of the *S*–He_1 and *S*–He_2 complexes are clearly seen as satellite bands on the parent transition, shifted by -6.5 and -13.0 from the stilbene origin. The equal successive shifts of these transitions from the parent transition point to the helium atoms taking up similar positions on the *t*-stilbene molecule. While we do not have the spectral resolution needed to directly determine the structure of the complex, past experience with other aromatic–rare gas complexes point to the helium atom being positioned above the plane of the stilbene molelcule where it can interact with the π orbital electrons of stilbene.

Stilbene–He_n transitions are also readily identifiable built on the strong progression in ν_{25} at 197 cm^{-1} (25_0^1) and 394 cm^{-1} (25_0^2). These transitions exhibit identical shifts from the parent transition (-6.5 cm^{-1} for *S*–He and -13.0 cm^{-1} for *S*–He_2) to those at the origin. Unfortunately, both the 25_0^1–He and 25_0^2–He transitions experience some interference from the 37_0^4 and $25_0^1 37_0^4$ parent transitions, respectively. However, at the highest backing pressure conditions used, the van der Waals transition can be made considerably larger than the parent transition. Under these conditions it is clear that both the 25_0^1–He and 25_0^2–He transitions possess rotational band contours which, at our resolution, are identical to those of the peaks built on the origin. The *S*–He_2 transitions built on 25_0^1 and 25_0^3 are free from interference and are also narrow in contour.

The dispersed fluorescence spectrum of the 25_0^1–He transition is shown in Fig. 2. The spectrum was taken under conditions where interference from the 37^4 parent level was insignificant. The peaks furthest to the blue (left) in the spectrum are due to resonance fluorescence from the initially excited level of the undissociated complex, i.e., 25^1–He. The other peaks arise from levels which are not so clearly identified. We will see in the next section that the excited state dissociation energy of the stilbene–He complex is less than 47 cm^{-1}. Thus, the complex excited to 25^1 has energy far in excess of the dissociation threshold and we would expect that the emission we observe is from the stilbene parent molecule following vibrational predissociation. Direct lifetime measurements on several of these peaks by Semmes *et al.*[19] (hereafter referred to as SBZ) confirm this assumption, yielding free stilbene emission rise times of 156 ps. The only levels below 150 cm^{-1} in the fluorescence excitation spectrum involve the two out-of-plane phenyl ring modes ν_{36} and

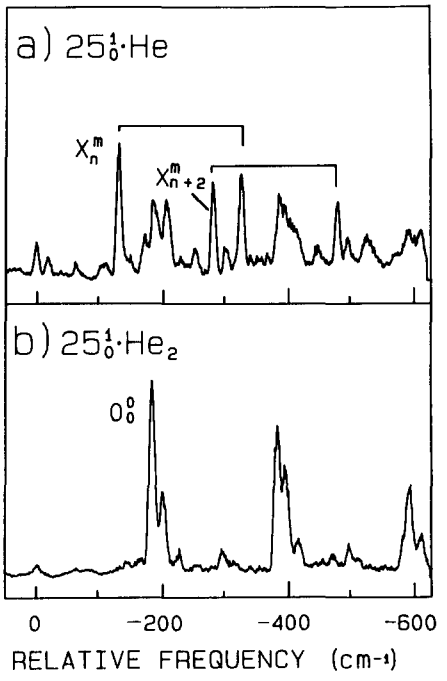

FIG. 2. Dispersed fluorescence spectrum of the 25_0^1–He transition. The peaks furthest to the blue in the spectrum are resonance fluorescence from the initially excited 25^1–He level. The X_n^m transition is an unassigned parent transition following dissociation of the complex. The tie lines indicate the positions of the 25_1^0 transition built on the X^m peaks.

ν_{37}; i.e., 0^0, 36^1, 37^1, 36^2, $36^1 37^1$, 37^2, 36^3, $36^2 37^1$, $36^1 37^2$, and 37^3. We have recorded the dispersed fluorescence spectra from all these levels and have eliminated all of them as possible sources of the emission we observe, except for the 0^0 level which may be a minor channel at most. SBZ also recognized this quandary and ascribed the observed peaks to dark states reached by IVR in the complex. We concur that the observed emission must be from levels which, if they are allowed at all, are only very weakly present in the absorption spectrum arising from the zero point level of the ground state. Thus, this level or levels must be either very weak a_g levels or fundamentals of a_u,b_u, or b_g symmetry. We have carried out an extensive search for the X_0^1 (in the case of a weak a_g mode) or X_0^2 transitions by taking dispersed fluorescence spectra of any parent transitions in these regions of the fluorescence excitation spectrum whose identity is not known with certainty.[16] Unfortunately, we have not been able to identify the responsible parent transition from this search. The observed dispersed fluorescence spectrum is a sparse one. In particular, it shows little or no activity in ν_{37}, indicating little or no coupling between the new vibration and the out-of-plane phenyl ring torsion. The dispersed fluorescence spectrum of the 25_0^2–He transition is very similar to that from 25_0^1–He, just shifted from the latter by one quantum in ν_{25}, i.e., the major transitions would be $25_0^1 X_n^m$ and $25_0^1 X_{n+2}^m$.

In summary, the helium van der Waals transitions built on the in-plane vibrations 25^1 and 25^2 are easily identifiable, narrow, unshifted, and vibrationally predissociate to form a new stilbene level or levels which are not accessible in absorption and are not coupled with out-of-plane vibrations of stilbene. The 0^0 product level is a minor channel at most.

2. Out-of-plane vibrations: $36_0^1 37_0^1$ and 37_0^2

a. Fluorescence excitation spectra: By contrast to these easily identifiable van der Waals transitions at the origin, the van der Waals transitions built on $36_0^1 37_0^1$ and 37_0^2 are much less obvious, appearing with peak intensities far lower than expected relative to their counterparts built on the origin. Interestingly, these trnsitions show substantial broadening by comparison to those at the origin, 25_0^1, and 25_0^2. The peaks are roughly 3 cm^{-1} FWHM, three times broader than any other feature in the spectrum of Fig. 1. The broadening is more clearly seen in the close-up scan around these transitions shown in Fig. 3(a).

The $25_0^1 36_0^1 37_0^1$ (279 cm^{-1}) and $25_0^1 37_0^2$ (292 cm^{-1}) stilbene–He van der Waals transitions are also about three times broader than those associated with the in-plane vibrations. Unfortunately, these transitions suffer from partial interference with parent transitions. Despite this, there is little doubt that the van der Waals transitions are broad, suggesting that the broadening is a mode-selective phenomenon restricted to the out-of-plane vibrational modes. The broadening cannot be ascribed to chance interference with stilbene parent transitions. In succeeding sections we will describe experiments which point unambiguously to the stilbene–He complex as the sole source of the broadened contour we observe.

b. Dispersed fluorescence spectra from the peaks of the transitions: In Fig. 4 we present the dispersed fluorescence spectra from the peak of the broadened $36_0^1 37_0^1$ and 37_0^2 stilbene–He transitions. The emission from $36_0^1 37_0^1$–He transition is almost exclusively from the 0^0 level of the parent, as has been reported previously.[19,20] Thus, on a time scale fast compared to fluorescence (2.7 ns), predissociation of the complex has occured. The two very small peaks just to the left of the origin emission are due to residual resonance fluorescence from the $36^1 37^1$ level of the undissociated complex.

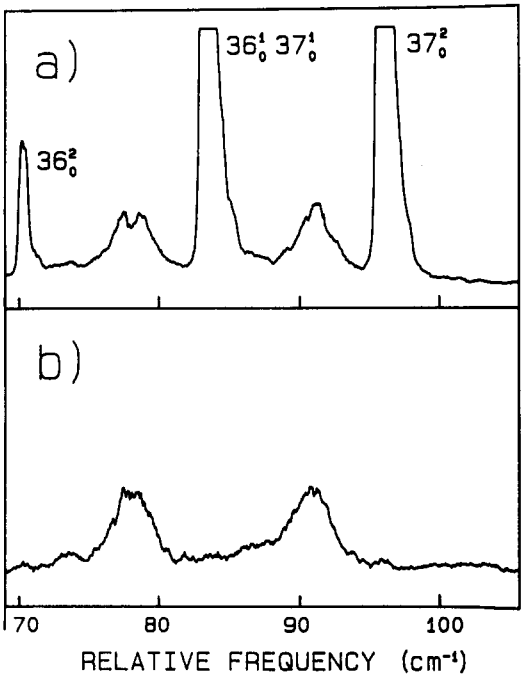

FIG. 3. (a) Close-up fluorescence excitation spectrum in the region of the broadened $36_0^1 37_0^1$–He and 37_0^2–He transitions when collecting the total fluorescence. (b) Corresponding wavelength-resolved excitation scan taken with fluorescence detection restricted to a 6 cm^{-1} band around the origin of the parent stilbene molelcule. The relative frequency scale has as its zero frequency position the origin of the stilbene parent molecule.

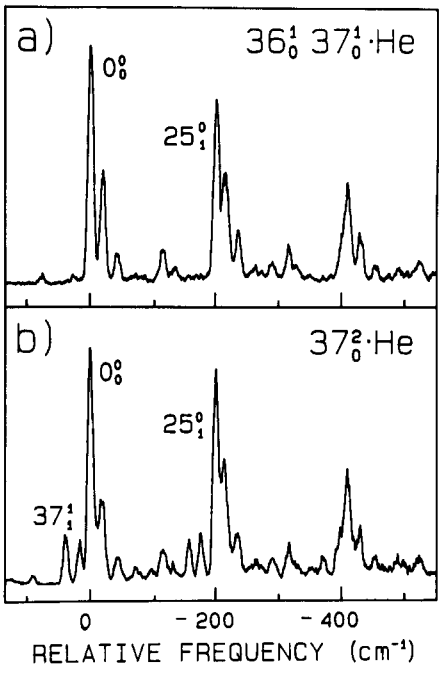

FIG. 4. Dispersed fluorescence spectra from the peaks of (a) the broadened $36_0^1 37_0^1$–He transition and (b) the broadened 37_0^2–He transition. In both cases the dominant fluorescence is from the zero point excited state level of the parent stilbene molecule following dissociation of the complex. The 37_0^2–He transition also forms stilbene in the 37^1 level to a small extent.

The dispersed fluorescence spectrum from the peak of the 37_0^2–He transition is shown in Fig. 4(b). As for the $36_0^1 37_0^1$–He transition, the spectrum is dominated by emission from the origin of the parent molecule following dissociation of the stilbene–He complex. However, here in addition we see emission from the 37^1 level of the stilbene parent which is the source of the two peaks just to the left of the origin (the 37_1^1 and 37_3^1 transitions). Observation of this channel[19] places an upper bound on the dissociation energy of the excited state stilbene–He complex of $D_0 = 47$ cm^{-1}. It is worth noting that the corresponding channel involving loss of one quantum of ν_{37} (i.e., the 36^1 product) is not present in the spectrum of $36_0^1 37_0^1$–He.

c. Wavelength-resolved excitation scans: Because elimination of congestion from other species is so important to our understanding of the cause and extent of the broadening we observe, we decided to carry out the following experiment to help rule it out as a possibility. We just observed that the fluorescence from the peak of both broadened transitions was dominated by emission from the origin of the parent molecule. Because of this fact, we can select for emission from predissociating stilbene–He complex by taking an excitation scan around the region of these broadened transitions with the monochromator tuned to detect emission only from

a small wavelength region around the 0_0^0 transition of the parent molecule. This will suppress emission from all other sources and in so doing allow us to clearly observe the true band shape of the broadened transitions. Figure 3(b) shows such a scan focusing on the broadened stilbene–He transitions. Note that the wavelength-resolved peaks are fully as broad as the total fluorescence detection scan above it. Thus, we conclude that the source of the broadening is not simply due to overlapping peaks from other complexes or stilbene transitions, but true mode-selective broadening characteristic of the stilbene–He complex.

Figure 5 presents wavelength-resolved excitation scans which extend further red than that in Fig. 3(b). We see in this figure that there are two additional broadened peaks red shifted from the major broadened peaks. The two scans were taken under different helium backing pressure conditions. In the upper trace the stilbene–He_2 population is less than 10% of the stilbene–He_1 population while the lower trace was taken under conditions where the stilbene–He_2 population was over 25% of stilbene–He_1. Note that the relative size of the two smaller, red-shifted peaks has not changed with respect to the primary broadened peaks at 78 and 90 cm^{-1}over this concentration range, although the overall contour has grown at higher backing pressure as one would expect. The only clear change in the spectra is due to the small interference apparent in Fig. 5(a) from the stilbene parent transitions at 70, 82, and 95 cm^{-1} which are masked by the larger size of the broadened transitions of Fig. 5(b). Thus we conclude that the entire band contour of Fig. 5(b), stretching from 57 to 93 cm^{-1} is due to transitions of the stilbene–He complex.

The peak at 65 cm^{-1} in Fig. 5 is 13 cm^{-1} red shifted from the $36_0^1 37_0^1$–He transition. This is precisely the separation between the $36_0^1 37_0^1$ and the much weaker 36_0^2 parent

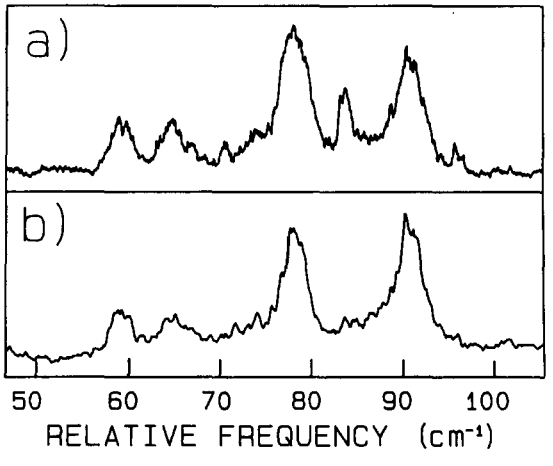

FIG. 5. Close-up wavelength-resolved fluorescence excitation spectra of the $36_0^1 37_0^1$–He and 37_0^2–He transitions under expansion conditions in which (a) the stilbene–He_2 population in the jet is less than 10% of stilbene–He population, and (b) the stilbene–He_2 population in the jet is 25% of the stilbene–He population. Note that the entire band contour from 57 to 93 cm^{-1} is hardly effected by the change. The small peaks which grow in at 70, 82, and 95 cm^{-1} in (a) are small interferences from the 36_0^2, $36_0^1 37_0^1$, and 37_0^2 parent transitions.

transitions. We thus tentatively assign the broadened peak at 65 cm^{-1} to 36_0^2–He. Two comments should be made. First, the 36_0^2–He peak appears to be fully as broad as the 37_0^2–He and $36_0^1 37_0^1$–He transitions. Thus, both out-of-plane phenyl ring motions, the ethylenic carbon–phenyl bend (ν_{36}) and the ethylenic carbon–phenyl torsion (ν_{37}) are strongly and selectively coupled to the background states producing the broadening. Second, the 36_0^2–He transition is several times more intense, relative to $36_0^1 37_0^1$ and 37_0^2, in the stilbene–He complex than in the bare stilbene molecule. We conclude that the 36_0^2–He transition is borrowing intensity from the higher oscillator strength ν_{37} transition upon complexation to helium. We are thereby invoking the background states as mediators of coupling between two out-of-plane phenyl ring motions, ν_{36} and ν_{37}. We have not been able to assign the second small, broadened peak located at 59 cm^{-1} in Fig. 5.

Clearly, transitions involving ν_{36} and ν_{37} in the stilbene–He complex are coupled very strongly with other levels available to the complex. This is very surprising given the fact that these transitions are less than 100 cm^{-1} above the origin. Since we are above the dissociation threshold, the states we access with the laser are imbedded in the dissociation continuum. However, direct coupling with this continuum cannot account for the breadth of these transitions since vibrational predissociation lifetime broadening of these peaks[19] should add no more than about 0.2 cm^{-1} to the width of the transitions. Since we are only 90 cm^{-1} above the origin and are accessing two of the lowest vibronic energy levels of the stilbene chromophore, the states to which the out-of-plane stilbene modes are so strongly coupled must be van der Waals levels associated with either out-of-plane (stretching) and/or in-plane (bending) motions of the helium atom.

d. Dispersed fluorescence spectra from the broadened contour: Due to the fact that the broadened transitions we are studying are stretched over some 30 cm^{-1}, we decided to take dispersed fluorescence spectra at other positions in the contours in addition to those at the top of the major peaks presented earlier. In Figs. 6(a)–6(c) we present three such scans which were taken over the comparatively short range from 88 to 93 cm^{-1} above the origin, respectively. Figure 6(b) was taken at the peak of the 37_0^2 transition, while Figs. 6(a) and 6(c) were taken on the red and blue edges of this peak. Note the dramatic change in the relative ratios of the $37^1/0^0$ stilbene product intensities over this region. While other groups have reported[21,22] the dispersed fluorescence from the 37_0^2–He transition, this sharp wavelength dependence to the emission was not recognized previously. Clearly even over the 5 cm^{-1} range spanned by these dispersed fluorescence spectra the character of the states giving rise to the emission is changing dramatically. *Thus, the broadening we observe is inhomogeneous broadening due to interaction with a comparatively dense set of levels.*

We have taken a total of 26 dispersed fluorescence scans over the region from 57 to 93 cm^{-1} above the origin. In all these scans the only emission we observe is from the 0^0 and 37^1 levels of the parent stilbene molecule following dissociation of the complex. However, below 80 cm^{-1} we can only observe emission from the 0^0 level to within our signal-to-

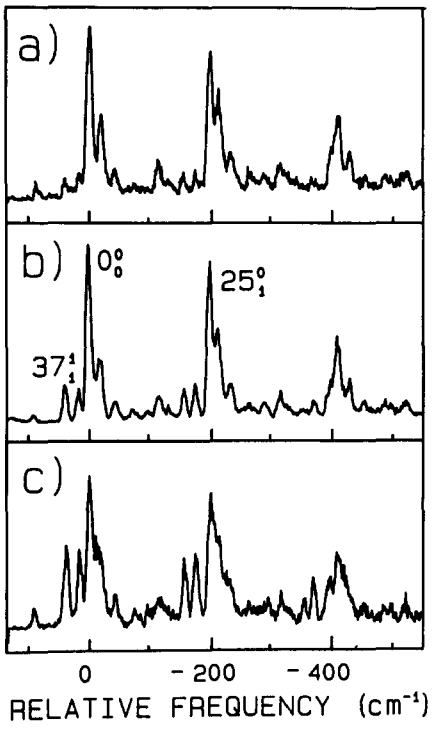

FIG. 6. Dispersed fluorescence spectra taken at three positions in the major broadened 37^2_0 transition. Excitation frequencies are (a) 88, (b) 90, and (c) 93 cm^{-1} above the origin. Note the dramatic change in the fraction of the emission due to the 37^1 level as one proceeds from (a)–(c).

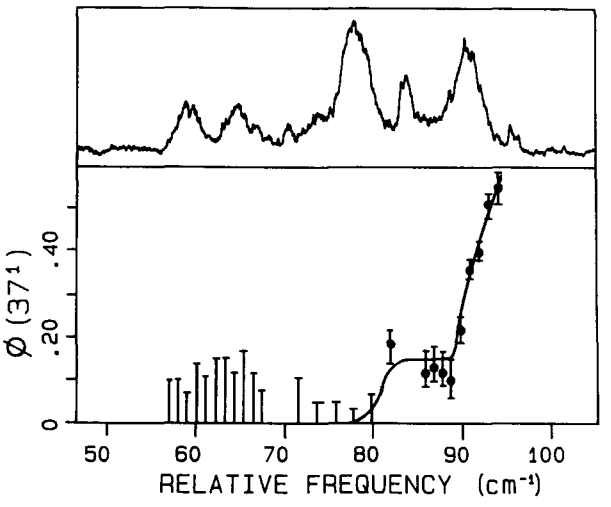

FIG. 7. A plot of the quantum yield of 37^1 production as a function of the excitation frequency over the broadened $36^1_0 37^1_0$–He and 37^2_0–He contours. The error bars below 80 cm^{-1} in the figure denote upper bounds on the fractional 37^1 population since in these spectra only the 0^0 level is observed to within our signal to noise.

noise ratio. Since we have only two product channels, we can summarize our data concisely by plotting the fraction of the total product molecules ending up in 37^1, $\phi(37^1)$, vs relative frequency. In order to determine this fraction we must (i) choose diagnostic transitions for the 37^1 and 0^0 product channels (e.g., 37^1_1 and 0^0_0, respectively), (ii) determine the relative fractions of the total emission from the levels represented by the diagnostic transitions, and (iii) determine the relative intensities of the diagnostic transitions as a function of relative frequency.[11,13] The results for $\phi(37^1)$ are presented in Fig. 7. The figure shows quantitatively just what we indicated qualitatively earlier. Below 80 cm^{-1} we do not observe any 37^1 emission. Error bars shown on the graph in this region represent upper bound estimates for $\phi(37^1)$ and are generally about 10% of the total product yield. These bounds become much more stringent in the region of the major peak at 78 cm^{-1}, at the peak of the $36^1_0 37^1_0$–He transition. There appears to be two regions to the graph when 37^1 is present: a flat, small probability region from 82–89 cm^{-1} and a sharply rising section as one tunes across the major 37^2_0 -correlated peak above 89 cm^{-1}. In Sec. IV we will address the possible causes of this changing product state distribution more fully.

e. Internal clock lifetime measurements: Recall that the dispersed fluorescence spectrum taken at the peak of the $36^1_0 37^1_0$–He transition [Fig. 4(a)] contained a very small amount of resonance emission from the undissociated $36^1_0 37^1_0$–He complex. The relative intensities of the diagnostic transitions due to the dissociated (0^0) and undissociated ($36^1 37^1$–He) complex can be used to obtain a rough measure of the lifetime of the level toward vibrational predissociation. Such measurements are referred to as internal clock measurements[11,13] of vibrational predissociation lifetimes since they make use of the known fluorescence lifetime of the parent molecule to internally calibrate the fluorescence intensities observed. In the present case the calculation affords a comparison with the elegant direct measurements by SBZ of the product stilbene (0^0) rise time from the peak of the $36^1_0 37^1_0$–He transition obtained using picosecond photo fragment spectroscopy.[19] These direct measurements yielded a value for the vibrational predissociation rise time of 34 ps. Here we measure the relative intensities of diagnostic transitions for the dissociated and undissociated complex, $I(36^1_0 37^1_0\text{–He})/I(0^0)$. The relative intensities are then combined with the known fluorescence lifetime of the stilbene molecule in this region of the spectrum ($\tau_{\text{rad}} = 2.7$ ns)[20] and the relative fraction of the total emission present in the diagnostic transition $[F(0^0)/F(36^1 37^1)]$ to obtain a rough measure of the lifetime of the level toward vibrational predissociation. As in the 37^2_0–He product yield measurements, long dispersed fluorescence scans from the 0^0 and $36^1 37^1$ levels of the parent have been used to estimate the fraction of the total emission intensity present in the diagnostic transitions. Combining these results,

$$\tau_{\text{VP}} = [\{I(36^1_0 37^1_0\text{–He})/F(36^1 37^1)\}/\{I(0^0)/F(0^0)\}]\cdot\tau_{\text{rad}}$$
$$= \{I(36^1_0 37^1_0\text{–He})/I(0^0)\}\cdot\{F(0^0)/F(36^1 37^1)\}\cdot\tau_{\text{rad}}$$
$$= \{0.035\}\{6\}\{2.7\text{ ns}\} = 0.6\text{ ns}.$$

Thus, our estimate based on fluorescence intensities seems to differ from the direct lifetime measurements by a factor of 20! We will see in Sec. IV that the internal clock measurements can be made consistent with direct measurements only if we drop the assumption made implicitly in the internal clock estimates that the vibrational predissociation and resonance fluorescence channels proceed directly *from the*

initially excited level carrying the oscillator strength in absorption.

3. Out-of-plane vibrations: $36_0^1 37_0^3$ and 37_0^4

Since the $36_0^1 37_0^1$ and 37_0^2 stilbene–He transitions proved to be so anomalous, we have attempted to identify and characterize the corresponding van der Waals transitions built on $36_0^1 37_0^3$ and 37_0^4. These have not been observed previously due to considerable interference with other transitions in this congested region of the spectrum. Figure 8(a) shows a close-up total fluorescence excitation scan of this region of the spectrum. There are three major parent transitions in this region: 25_0^1 at 197 cm^{-1}, 37_0^4 at 192 cm^{-1}, and $36_0^1 37_0^3$ at 180 cm^{-1}. The tie lines originating from these transitions denote the proposed positions of the corresponding stilbene–He van der Waals transitions. As noted previously, the 25_0^1–He peak is directly under the 37_0^4 parent transition while the 25_0^1–He_2 peak is clearly visible at 186 cm^{-1}. If the van der Waals shifts from the parent peaks were identical for all vibronic transitions, we would expect the 37_0^4–He peak to lie directly underneath the 25_0^1–He_2 transitions. Nevertheless, a careful look at the spectrum shows a peak located only 3.0 cm^{-1} red of the parent transition, as the tie line indicates. This peak possesses only half the shift the 0^0 or the in-plane 25^1–He transitions have with respect to their parent transitions (6.5 cm^{-1}). However, the major 37_0^2–He transition exhibited a shift of -5.5 cm^{-1}, and so we might expect yet a smaller red shift for the 37_0^4–He transition. Similarly, our tentative assignment for the $36_0^1 37_0^3$–He transition is the small peak -3.5 cm^{-1} from its parent transition. In Fig. 8(b) we present a wavelength-resolved excitation scan over the same region with the monochromator tuned to a 9 cm^{-1} band around the 0_0^0 transition of the parent stilbene molecule. Note that the suppression of parent transitions is not as complete as in the earlier scans. Furthermore, the congestion caused by the 25_0^1–He_n transitions which can also predissociate to form stilbene in the 0^0 level interferes with an unambiguous determination of the width and shape of the band contours of the $36_0^1 37_0^3$–He and 37_0^4–He transitions.

The dispersed fluorescence spectrum of Fig. 9 presents the most convincing evidence that the peak we have assigned the 37_0^4–He transition correctly. While the signal-to-noise ratio of this scan is not very good, we can observe two important features of the spectrum. First, the emission appears to be entirely from parent stilbene levels. Second, the two levels whose emission dominates the spectrum are 0^0 and 37^3. The presence of the 37^3 channel was confirmed by taking a dispersed fluorescence scan of the 37_1^3 stilbene hot band transition under the same conditions. The relative intensities and positions of the peaks identified in the spectrum, as well as the lack of a significant 37_3^3 peak, point to our assignment of this product channel as correct. There is evidence of some 37^2 emission in the spectrum as well, but it is less clear than the 37^3 peaks. The obvious conclusion we must draw is that the transition 3.0 cm^{-1} red of 37_0^4 is a transition due to a stilbene–X complex with dissociation energy less than 47 cm^{-1}. The only candidate for this complex is the stilbene–He complex.

The two major channels for the vibrational predissociation products are the smallest energy gap channel, 37^3, and the largest energy gap channel, 0^0. From the relative intensities we estimate that the 37^3 channel has a relative popula-

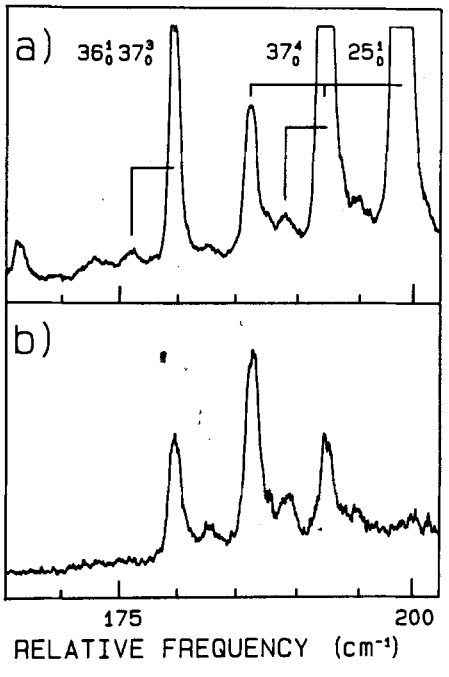

FIG. 8. Close-up fluorescence excitation spectra in the region near 25_0^1, $36_0^1 37_0^3$, and 37_0^4 taken under expansion conditions in which stilbene–He complexes are present in the jet. The tie lines in the upper figure denote the proposed positions of the stilbene–He_n transitions built on the levels to which they are tied. (a) Total fluorescence excitation spectrum. (b) Wavelength-resolved excitation spectrum in which fluorescence is detected only from a 9 cm^{-1} band centered around the parent stilbene origin emission. Note that there is still some interference from parent transitions in this scan.

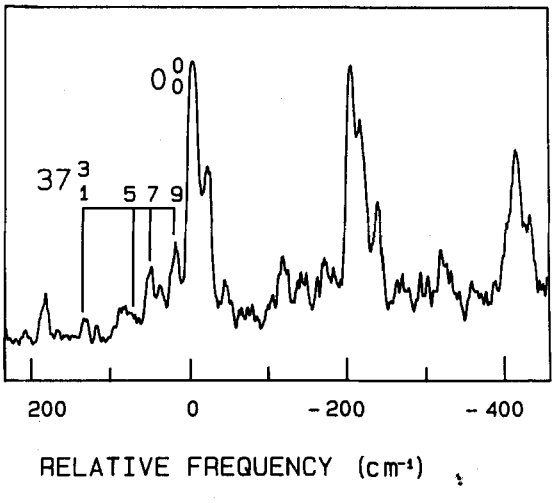

FIG. 9. Dispersed fluorescence spectrum of the 37_0^4–He transition. The major peaks are from the 0^0 level of the stilbene parent. As indicated in the spectrum, we can also identify peaks due to 37^3 by comparing the indicated peak positions and intensities with the dispersed fluorescence spectrum of the 37_1^3 hot-band transition of the stilbene parent molecule.

tion only about one-half that of the 0^0 channel. The dominance of the 0^0 channel occurs despite the presence of a large number of other channels which are energetically accessible to the products. Unlike the 37_0^2–He transition, there is no observable change in the relative fractions of these channels within the limited 3 cm^{-1} range of the band contour that we can probe free from interference.

The dispersed fluorescence spectrum of the $36_0^1 37_0^3$–He transition shows the predominance of the 0^0 channel as well. Unfortunately, the signal-to-noise ratio in this scan was too poor to provide definite conclusions about other product channels. *In summary, the* $36_0^1 37_0^3$*–He and* 37_0^4*–He transitions both tend to favor* 0^0 *channel product formation even though this channel presents the largest, not the smallest, energy gap.*

Note the stark contrast of these results involving out-of-plane vibrations with those of 25_0^1–He, an in-plane mode. The energies available to the stilbene–He complexes excited to 25^1 and 37^4 differ by only 3 cm^{-1} out of a total of 200 cm^{-1}. Yet, despite their near degeneracy, the product state distributions bear no resemblance to one another. The 25^1 level produces a new level or levels with energy between 103 and 150 cm^{-1} and very little 0^0 formation while excitation of the 37^4 level produces mostly 0^0 and some 37^3 stilbene products.

B. Stilbene–H_2

Replacing helium with hydrogen as the species complexed to stilbene offers interesting comparisons: while hydrogen is even lighter than helium, its far greater polarizability will give it significantly stronger binding to stilbene, likely far in excess of the 80–90 cm^{-1} needed to turn off predissociation from the $36_0^1 37_0^1$ and 37_0^2 levels. Both the lighter mass and stronger binding should increase the van der Waals vibrational frequencies and thus decrease the density of interacting states. An overview fluorescence excitation spectrum in the region of the origin taken with a 2% H_2 in helium mixture serving as expansion gas is shown in Fig. 10. The stilbene–H_2 origin is clearly visible in the spectrum, shifted 28 cm^{-1} red of the parent transition. The stilbene–$(H_2)_2$ origin is located at -57 cm^{-1}, once again pointing to similar positions for the two hydrogen molecules (one on either side of the stilbene plane?) in that complex. For ease of comparison of the various complexes, the shifts of the complex transitions from the corresponding parent transitions for the complexed species studied in this work is summarized in Table I. The 25_0^1–H_2 and 25_0^2–H_2 transitions (not shown in the figure) are also red shifted 28 cm^{-1} from their parent transitions and both have identical band contours to that at the origin. By contrast, the $36_0^1 37_0^1$–H_2 and 37_0^2–H_2 transitions are much reduced in *peak* intensity (as were the corresponding stilbene–He transitions) instead exhibiting a dense set of closely spaced peaks. This region is expanded for closer inspection in Fig. 11(a). The 37_1^1 and 36_0^2 transitions

TABLE I. Stilbene–X complex shifts and vibrational frequencies.

X	0^0_{shift} [a]	ν'_{36}	ν'_{37}	ν'_{25}	ν''_{36}	ν''_{37}	ν''_{25}
···	0	34.8	47.7	197	57	9	200
He	−6.5	35.3	48.2	197	57	8	200
H_2	−28	33	42	198	58	8	200
Ne	−16	25[b]	49[b]	200	59	6	202
Ar	−63	33[b]	40[b]	···	62	⩽3	205
He_3	−13.0						
He_3	−19.8						
$(H_2)_2$	−57						
Ar_2	−132						

[a] Shift from the origin of the parent stilbene molecule in wave numbers.
[b] Based on our tentative excited state assignments.

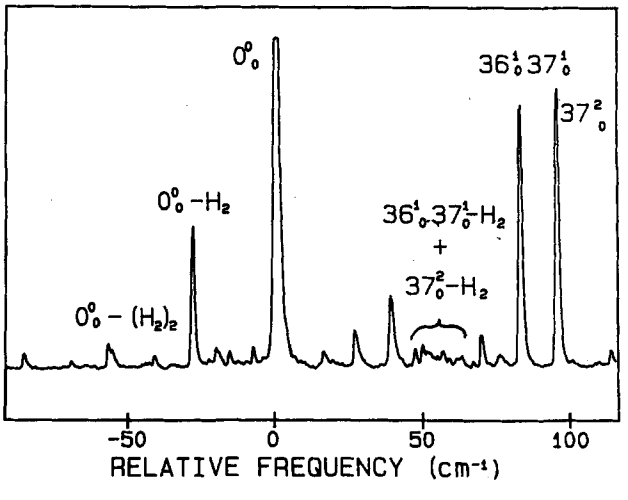

FIG. 10. Total fluorescence excitation spectrum in the region near the origin taken with a 2% hydrogen in helium expansion mixture. Note the dense structure associated with the $36_0^1 37_0^1$–H_2 and 37_0^2–H_2 transitions.

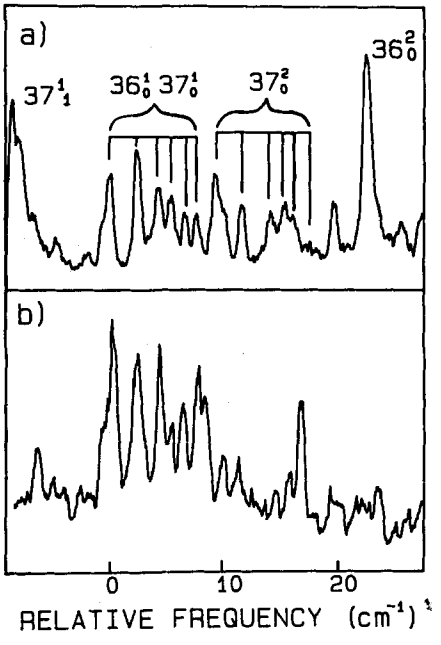

FIG. 11. Close-up fluorescence excitation spectrum (a) in the region of the $36_0^1 37_0^1$–H_2 and 37_0^2–H_2 transitions, and (b) in the region of the $25_0^1 36_0^1 37_0^1$–H_2 and $25_0^1 37_0^2$–H_2 transitions. The tie lines indicate the substructure we have assigned to the $36_0^1 37_0^1$ and 37_0^2 transitions.

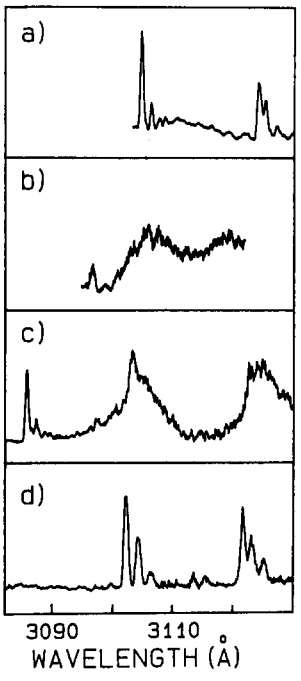

FIG. 12. Dispersed fluorescence spectra of (a) the 0_0^0–H_2 transition, (b) one of the closely spaced 37_0^2–H_2 transitions, (c) the 25_0^1–H_2 transition, and (d) one of the closely spaced $25_0^1 36_0^1 37_0^1$ transitions. See the text for a discussion of these spectra.

marked in the figure are parent transitions. The rest of the structure can be ascribed to the stilbene–H_2 complex since it (i) scales with the stilbene–H_2 transition at the origin, (ii) is present in its entirely when only the stilbene–H_2 complex is present significantly in the jet, and (iii) disappears in the absence of H_2 in the jet. The likely assignments of the peaks to either $36_0^1 37_0^1$ or 37_0^2 are given in the figure. This assignment is based on position relative to the parent transitions and also the similarity of the dense structure built on the lowest energy levels indicated by the tie lines in the figure.

Figure 11(b) shows the corresponding structure associated with the $25_0^1 36_0^1 37_0^1$–H_2 and $25_0^1 37_0^2$–H_2 transitions. Note the overall similarity of the dense structure with that above it, namely, the $36_0^1 37_0^1$–H_2 and 37_0^2–H_2 transitions. The major difference is that the $25_0^1 37_0^2$ grouping is slightly further red-shifted than the 37_0^2 grouping. This similar spacing of these transitions reasons for the out-of-plane levels all being coupled to the same set of states which are borrowing oscillator strength from the out-of-plane levels.

In Fig. 12 we present a series of dispersed fluorescence spectra of the stilbene–H_2 complex taken at (a) the origin, (b) one of the 37_0^2 peaks, (c) 25_0^1, and (d) one of the $25_0^1 37_0^2$ peaks. At the origin [Fig. 12(a)] we see a dispersed fluorescence spectrum nearly identical to that of the parent origin except shifted 28 cm^{-1} red of the parent spectrum. On the other hand, the $36_0^1 37_0^1$ and 37_0^2 peaks all show completely unresolved spectra like that shown in Fig. 12(b). These spectra are low signal-to-noise spectra both due to the reduced intensity of the transitions in absorption and to the broad nature of the dispersed emission. In Fig. 12(c) we see the 25_0^1–H_2 dispersed fluorescence spectrum. Interestingly, this spectrum appears as a combination of the two above it, exhibiting both some structured and some broadened regions of the spectrum. In particular, the resolved peaks on the left of the spectrum are resonance fluorescence from the 25_0^1–H_2 transition which carries the oscillator strength in absorption from the vibrationless ground state. The broadened emission is centered near the 0_0^0 and 25_1^0 levels of the complex emission [see Fig. 12(a) above it] but appears in wide bands of about 50 cm^{-1} breadth. Such broadened emission has been observed in the dispersed fluorescence spectra of other complexes.[10,11] It has been ascribed in these cases to IVR to the van der Waals modes of the complex. A similar interpretation has been given to dispersed fluorescence spectra in large isolated molecules where the background levels are low energy intramolelcular levels.[21] In the present case, the 25^1–H_2 levels carrying the oscillator strength are coupled to a dense set of van der Waals levels which are isoenergetic with them. The ratio of structured to broadened emission intensity then gives a measure of the extent of mixing of the 25_0^1–H_2 levels with the background van der Waals levels. The major source of van der Waals state density comes from the lowest intramolecular vibronic levels of the chromophore molecule (i.e., the 0^0 level) so that the emission from these levels is centered around the origin-like emission wavelengths but is broadened due to the slightly different transition wavelengths of these van der Waals levels (0^0–vdW^n) to levels in the electronic ground state of the complex. For the 25_0^1–H_2 transition, the presence of such extensive mixing with background levels ($\sim$10% structured/unstructured emission) despite no apparent change in the rotational band contour in excitation points to a quite high density of interacting states already 200 cm^{-1} above the zero-point level in the excited state.

In Fig. 12(d) we show the dispersed fluorescence spectrum of one of the dense set of peaks associated with $25_0^1 37_0^2$–H_2. By comparison to (b) and (c) above it this spectrum is structured and characteristic of emission from the 0^0 level of the parent stilbene molecule. Thus, by 280 cm^{-1} above the origin of the complex we have exceeded the binding energy of the stilbene–H_2 ccomplex so that vibrational predissociation occurs from this level. The fact that the 25_0^1 level shows no dissociated complex points to the 25^1–H_2 level being below the dissociation threshold. Thus, the excited state binding energy of the stilbene–H_2 complex is bracketed between 197 and 273 cm^{-1} (Table II).

The comparison of Figs. 12(b) and 12(c) is particularly important for our understanding of the mode selective coupling to the van der Waals bending modes. While Fig. 12(c) shows significant resonance fluorescence from the original

TABLE II. Excited state binding energies of several of the stilbene–X van der Waals complexes.

Complex	Excited state binding energy D_0
Stilbene–He	$\leqslant 49$ cm^{-1}
Stilbene–H_2	$197 \leqslant D_0 \leqslant 273$ cm^{-1}
Stilbene–Ne	$88 \leqslant D_0 \leqslant 150$ cm^{-1}

25^1 level carrying the oscillator strength, the 37^2 level shows no such resonance fluorescence even though it is 2.5 times lower in energy. *Thus, it appears that intramolecular–intermolecular state mixing is a highly mode-selective process which is enhanced by out-of-plane vibrational excitation even when vibrational predissociation is not energetically accessible to the complex.* The excitation spectrum exhibits this mode selectivity in the splitting of the $36_0^1 37_0^1$–H_2 and 37_0^2–H_2 levels into a dense of transitions spaced by only 1 cm^{-1}. The dispersed fluorescence spectra provide additional evidence by the complete broadening of the emission from these levels even though the much higher energy 25_0^1–H_2 level retains some structured resonance fluorescence.

The dense, repeated structure of the stilbene–H_2 transitions built on these out-of-plane stilbene modes appears to be the result of changing transitions with strong $\Delta v_{\text{bend}} = 0$ Franck–Condon factors for in-plane motions into a set of 5–6 strong $\Delta v_{\text{bend}} > 0$ transitions when out-of-plane vibrational motion is excited. Each of these individual transitions in stilbene–H_2 can support further extensive state mixing and thus each must be coupled to an even higher density of background states. Our hypothesis is that the closely spaced levels are a progression in the van der Waals bend whose vibrational frequency in stilbene–H_2 is only about 1 cm^{-1}(!). This is one to two orders of magnitude smaller than the bending mode vibrational frequencies typical of other aromatic–X van der Waals complexes.[22,23]

The obvious difference between aromatic systems such as benzene or tetrazine and the *trans*-stilbene molecule is that the *trans*-stilbene molecule possesses an aromatic system which extends over both phenyl rings of the molecule. The aromatic system is thus spread over the entire 10 Å length of the molecule and the bending mode vibrations could in principle involve H_2 motion over this entire 10 Å length. *As we will show in Sec. IV, such delocalization of the complexed H_2 molecule over the two phenyl rings of trans-stilbene can account for both the anomalous state density and low vibrational frequencies we observe.* This bending mode structure was not resolved in the corresponding stilbene–He transitions like it is here. However, the close similarity of these system makes it quite natural to assume that a similar set of states, merely unresolved, is responsible for the broadening and the red-shaded tail apparent in that system.

C. Stilbene–Ne and stilbene–Ar

The stilbene–Ne and stilbene–Ar complexes have been studied in much the same fashion as the stilbene–He and H_2 complexes already discussed. Unfortunately, it is difficult to make the stilbene–Ne and stilbene–Ar complexes at high concentration free from a broad background due to higher complexes. As a result, we will only summarize our observations briefly. The tentative assignments for the ground and excited state vibrational frequencies for these complexes are given in Table I. Table II places bounds on the stilbene–Ne binding energy taken from dispersed flourescence spectra of this complex. Figure 13 shows the fluorescence excitation spectrum of the stilbene–Ar complex. Two features of the spectrum stand out. First, unlike the stilbene–He and stilbene–H_2 spectra, this spectrum is replete with a large number of van der Waals transitions[24,25] built on the origin. We have indicated the probable members of the van der Waals bending and stretching progressions by tie lines extending from the origin of the complex. Second, the tentatively assigned $36_0^1 37_0^1$–Ar and 37_0^2–Ar transitions (marked by asterisks in the figure) are shifted, but do not appear broadened relative to the in-plane transitions. It is interesting that the narrowing in the out-of-plane transitions occurs for the same complex for which the strong van der Waals structure appears built on the origin. At least some of this structure is probably bending mode structure, and indicates a significant increase in frequency from that seen in stilbene–H_2, probably resulting from the localization of the argon atom on a single phenyl ring.

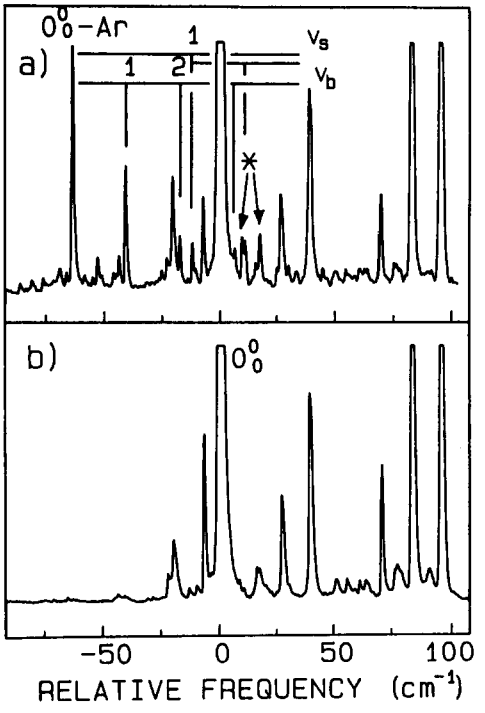

FIG. 13. Total fluorescence excitation spectra of the region near the $S_1 \leftarrow S_0$ origin with (a) a 1% Ar in helium expansion mixture, and (b) under identical expansion conditions but with no argon flowing. The tie lines indicated the tentative assignments of the van der Waals structure built on the origin. The peaks marked by an asterisk are those we have tentatively assigned as the $36_0^1 37_0^1$–Ar and 37_0^2–Ar transitions.

IV. DISCUSSION

A. The source of the high density of interacting states: Delocalization of the complexed species

We have already alluded in the results section to a very fundamental puzzle presented by the mode-selective broadening we observe, particularly in the stilbene–He complex; namely, how we can generate a high enough density of states to account for the broadening we observe less than 100 cm^{-1} above the origin in the excited state. This is such a small excess energy that conventional wisdom would say that the density of bound states should be far too low to act as a bath of several states per cm^{-1}. We have already noted the major source of the high density of states: the van der Waals bending modes. Due to the light mass of the helium atom, the

normal mode motion of the in-plane van der Waals bend involves motion of the helium atom along, but above the plane of, an immobile stilbene molecule. If the complexed species were localized above one of the phenyl rings, it would have a bending frequency much like that of other aromatic–rare gas complexes (e.g., $\sim 20\ cm^{-1}$ for X = Ar).[23] However, in the extreme case of complete delocalization of the helium atom over the π framework of stilbene, the complexed species will move in a nearly flat-bottomed potential which will allow it to sample both phenyl rings during its oscillation. The distance between the centers of the two phenyl rings is about 7 Å, while the end-to-end distance of the molecule along its long in-plane axis is about 10 Å. Thus, we hypothesize that in stilbene–He the "long axis" bending mode is really more a pseudotranslation within a long, one-dimensional square well than it is a simple harmonic oscillator. The narrow band contours of the stilbene–He origin and in-plane transitions point to strong $\Delta v_{\text{vdW bend}} = 0$ Franck–Condon factors (FCF) in these cases. However, when out-of-plane phenyl ring modes are excited in the stilbene chromophore, the additional out-of-plane motion of the phenyl rings modifies the potential energy surface in which the helium atom moves. The result is a changed set of van der Waals bend FCFs for these levels which now spreads the 36_0^2,$36_0^1 37_0^1$, and 37_0^2 oscillator strength over a series of van der Waals bending modes (i.e., $\Delta v_{\text{vdW bend}} > 0$) of frequency sufficiently small that we cannot resolve the individual transitions in our experiment. If we treat the van der Waals bend as a pseudotranslation in a one-dimensional square well, then near the bottom of that well the van der Waals state density is about 2–3 states per cm^{-1}, sufficiently high to account for the unresolved broadening we observe.

The stilbene–H_2 data lends considerable support to this hypothesis. In this complex the lighter mass of H_2 and its stronger interaction with the ring lead to an increase in the pseudotranslation frequency to the point where individual van der Waals levels are now resolvable in our excitation spectrum (Fig. 11). The approximate spacing within the group of stilbene–H_2 transitions built on $36_0^1 37_0^1$ and 37_0^2 is about 1 cm^{-1}, pointing to a 1 cm^{-1} van der Wasls bending vibrational frequency. This spacing is remarkably close to the 0.8 cm^{-1} spacing we calculate for the H_2 mass moving in a square well of 10 Å length ($\Delta E = h^2/2mL^2$). The observed transitions in the excitation spectrum, then, should be viewed as a van der Waals bending mode progression built on $36_0^1 37_0^1$. Again, by contrast, when in-plane motions are excited, even though this same van der Waals level structure is likely still present, the narrow, unshifted van der Waals transition suggests strong $\Delta v_b = 0$ Franck–Condon factors due to a weak coupling between the two motions.

Note that the spacing of the closely spaced structure indicated by tie lines in Fig. 12 is not uniform, but varies as 2.4, 1.8, 1.1, 1.1, and 1.0 cm^{-1}. If this structure can all be ascribed to the pseudotranslational motion of H_2 along the long, in-plane axis of stilbene, as we propose, then the decrease in level spacing to about one-half its original spacing is suggestive of tunneling[26] of the hydrogen molecule between a small barrier of about 3–5 cm^{-1}. The likely position of a barrier would be the region of the ethylenic carbons with the two wells located at the centers of the two phenyl rings, 7 Å apart.

The stilbene–Ne and stilbene–Ar complexes exhibit spectra which do not necessarily call for delocalization of the neon or argon atom. There are several potential reasons for this change from delocalization to localization. First, the increase mass of the argon atom will decrease the probability of tunneling caused by even a small potential barrier between the two phenyl rings. Second, the barrier height may be increased in stilbene-Ar due to the stronger interaction of the argon atom with the π orbital. Finally, the form of the in-plane normal mode motion will change with increasing mass of the complexed species as the weight of the complexed atom becomes more comparable to that of the phenyl rings. In the limit of a very heavy complexed atom one should better view the in-plane bend as a rotation of the phenyl ring about the heavy atom. This could be partially responsible for an increased barrier to motion between the phenyl rings.

So far, this discussion of delocalization has taken place without regard to some important experimental data[25] on the geometry of these stilbene–rare gas complexes. While the precise geometry is not known with certainty for any of the stilbene van der Waals complexes of interest here, Baskin *et al.*[25] recently used rotational coherence measurements to determine that the sum of the *B* and *C* rotational constants is significantly lower in the stilbene–He and stilbene–Ar complexes than in the parent molecule. Since the *B* and *C* axes of the complex lie perpendicular to the long in-plane axis of *t*-stilbene (the *A* axis), this result points to the complexed species lying off the *B* and *C* axes with its additional mass over the phenyl rings. This would seem to be at odds with our conjecture of delocalization of the helium atom or hydrogen molecule in the stilbene–He and stilbene–H_2 complexes (although it is consistent with our hypothesis of localization in stilbene–Ar). However, rotational constants reflect the vibrationally averaged structure of the complex. If we picture the in-plane motion of the helium atom as if it were a particle in a 10 Å one-dimensional square well, the root-mean-square displacement of the rare gas atom would be 2.9 Å, by comparison to 3.5 Å for the atom localized above the center of one of the phenyl rings.[18]

B. The strong coupling of the van der Waals states with out-of-plane phenyl ring motions

1. Some possible reasons for the strong coupling

We have so far concentrated on the source of the high density of states. Now we will focus on the strong, selective coupling of these states to the out-of-plane phenyl ring vibrations of the stilbene molecule. First, there are excellent kinematic reasons for the strong coupling of the out-of-plane phenyl ring motions with the motion of the complexed atom. As we pointed out previously,[15] the position of the complexed atom or molecule is above the plane of the molecule so that phenyl bending or torsional motion will involve motion directly against the van der Waals-bound species. In fact, we have become accustomed to calling these out-of-plane phenyl ring modes "paddleball" modes since the phenyl ring interaction with the complexed atom is much like

that of a racquet against a ball. Second, the small energy mismatch between the very low frequency, large amplitude phenyl ring motions and the van der Waals vibrations should enhance the coupling between the motions. Third, the delocalization of the helium atom or hydrogen molecule should facilitate strong coupling. In condensed media the possibility of multiple collisions between species provides an efficient route for deactivation of excess vibrational energy. Speaking classically, in our case the delocalized pseudotranslational bending modes involve the traversal of the complexed species back and forth over the 7 Å distance from one phenyl ring to the other. For a helium atom or hydrogen molecule with a few wave numbers of pseudotranslational kinetic energy, the time for traversal is on the order of a few picoseconds. This is the same time scale as the period of the phenyl ring oscillation for the out-of-plane torsional and bending modes. Thus the interaction between the two motions in these complexes may be viewed in some sense as multiple "collisions" of the two species on the picosecond time scale.

While such arguments are pleasing ones to make, we must be careful not to treat the coupling process here as a truly dynamical one involving energy flow from the intramolecular to the intermolecular levels, i.e., dynamic IVR. In this work we have proven the inhomogeneous nature of the stilbene-He band contours of the out-of-plane transitions (Sec. III A 2 d). Furthermore, with the 10 ns pulse duration of our laser we are incapable of preparing the coherent superposition of states which is required for a true, time-dependent energy transfer to occur to the van der Waals modes.[13,27,28] Instead, we must view laser excitation as preparing a mixed state containing partial van der Waals mode character at $t = 0$.

2. A two-tiered coupling scheme to the van der Waals modes

The combined results of the excitation spectra and dispersed fluorescence spectra point to the out-of-plane vibronic levels of the stilbene–X complexes being coupled to two tiers of background levels. This two-tiered coupling scheme is most clearly observed in the stilbene–H_2 complex. Recall that in the fluorescence excitation spectrum of this complex, the 37_0^2 transition is split into a set of 5–6 closely spaced peaks. The splitting is the result of strong coupling of the 37^2 level with a first tier of levels of nature $|37^2$–vdW bend$^m>$ where $m = 0$–5.

The effects of a second tier of coupled background levels are seen in the dispersed fluorescence spectra. When we disperse the fluorescence from each of the individual transitions of character $|37^2$–vdW bend$^m>$, we observe broadened emission centered around the positions of the major bands of the 0^0 level of the complex. Such broadening arises from state mixing with a second tier of levels resulting in partial 0^0–vdW^n character in the laser-prepared state. Due to the varied nature of the coupled van der Waals levels, the emission spectra of each 0^0–vdW^n state is slightly different. It is intriguing that the mixed levels appear to be primarily those built on the lowest intramolecular vibronic level of stilbene, the 0^0 level. The second tier state mixing is thus density-of-state dominated in this case; i.e., the mixed levels take on the characterof the background levels which produce the highest density of states at a given energy.

C. The relationship between vibrational predissociation and intramolecular–intermolecular state mixing

We now turn to the effect of the extensive state mixing on the vibrational predissociation process, focusing our attention on the stilbene–He complex. We wish to answer the question, "To what extent does the intramolecular–intermolecular state mixing effect the product state distribution observed when predissociation occurs, i.e., when coupling occurs to the dissociation continuum?"

The first hint that state mixing is affecting the predissociation process was seen in the changing predissociation product state distribution which occurs as we tune over the broadened 37_0^2 band contour (Fig. 7). Recall that over the range from 80–93 cm^{-1}, the fraction of products formed in the 37^1 level changes from less than 5% to over 50%. The majority of this rise occurs over the 3 cm^{-1} breadth of the 37_0^2 peak. One could interpret this sudden increase in $\phi(37^1)$ as the result of the complex overcoming an energetic threshold to the formation of 37^1. The 37^1 channel, if it were energetically allowed, would be the smallest energy gap, $\Delta v = -1$ channel. We estimate that just above threshold, this channel should have a vibrational predissociation rate several hundred times faster than the 0^0 product channel. Thus as this channel opens, it would be expected to compete successfully with the 0^0 channel. However, there are several difficulties with this interpretation. First, one must still account for the relatively long, flat section of the $\phi(37^1)$ curve in the red-shaded tail of the 37_0^2 peak from 82–90 cm^{-1}. Second, we have been unable to detect a similar turn on of the 36^1 channel from $36_0^1 37_0^1$ transition or the 37^3 channel from 37_0^4 like we should if it were purely an energetic threshold phenomenon. Third, the binding energy we deduce from this assumption is at odds with our results on the *p*-methyl-*trans*-stilbene–He complex presented in the adjoining paper. If the increase in $\phi(37^1)$ was the result of exceeding the binding energy of the complex, then $D_0' = 95\text{–}47.5 = 47.5\ cm^{-1}$. In the *p*-methyl-*trans*-stilbene–He complex, we would expect the addition of the methyl group to increase the binding energy of the helium atom in this complex, i.e., D_0'(*p*-methyl–He) $\geqslant 47.5\ cm^{-1}$. However, we see the $\Delta v = -1$ channel of ν_{37} showing up strongly in the dispersed fluorescence spectrum of one of the transitions in *p*-methyl–He even though the vibrational frequency of ν_{37} is reduced in *p*-methyl-*trans*-stilbene to 45 cm^{-1}, i.e., D_0'(*p*-methyl–He) $< 45\ cm^{-1}$. Thus the changing product state distribution in the 37_0^2 contour of stilbene–He is probably not due purely to energetic threshold effects.

Alternatively, the $\phi(37^1)$ variation may result from the changing nature of the mixed states accessed by the laser as we tune across the broadened contour. We have ascribed the broadening of the band contour to strong coupling to the van der Waals pseudotranslational modes spreading the 37_0^2 oscillator strength over a series of van der Waals transitions $|37^2$–vdW$^m>$ which are too closely spaced to be resolved.

The changing predissociation product state distribution is then simply reflecting the changed van der Waals character of the states accessed by the 0.3 cm^{-1} bandwidth laser. It is intriguing that "priming" the van der Waals complex with a small amount of van der Waals bend excitation has such a dramatic effect on the product channels chosen by the dissociating complex. It appears that, with increasing van der Waals bend excitation in the doorway state (as we tune from red to blue across the 37_0^2 contour), the complex increasingly selects the smaller energy gap product channel.

The effect of state mixing on predissociation is also seen in a comparison of our internal clock lifetime measurements with the direct measurements[19] of vibrational predissociation product rise times for these levels in the stilbene–He complex. Recall that the internal clock lifetime we estimated for the 36^137^1 level was a factor of 20 different from the actual predissociation lifetime. However, as other authors have noted,[11,13] internal clock estimates of rates for processes hinge on a critical assumption; namely, that the processes which occur following excitation all occur as *single step processes from the same state.* From what we have already said, the out-of-plane phenyl ring levels we access with the laser possess considerable van der Waals character. As Ewing has pointed out,[29] intramolecular–intermolecular state mixing can greatly affect the vibrational predissociation lifetimes by providing much smaller energy gap channels for the predissociation process. Such Fermi resonance has been used by Butz *et al.*[11] to account for the much larger-than-expected 0^0 predissociation channel observed from several excited state levels in the *p*-difluorobenzene–Ar complex. Similar arguments can be used here to account for the apparent discrepancy between our results and those of SBZ.[19] If we view predissociation as occuring directly from the 36^137^1 level carrying the oscillator strength in absorption; namely,

$$S(36^137^1)\text{–}He \xrightarrow{k_{vp}} S(0^0) + He, \tag{1}$$

then our estimate of the vibrational predissociation lifetime based on the internal clock measurements is 20 times slower than the direct measurement. However, now we instead assume that predissociation is occuring from a set of rovibronic states each of which possesses partial 36^137^1 character (P) and partial background vibronic character ($1\text{-}P$). The primary coupling of the 36^137^1 level is with the first tier of van der Waals pseudotranslational modes. A second tier of van der Waals levels also exists built on lower lying stilbene vibronic levels. Our 0.3 cm^{-1} bandwidth laser accesses a large number of rovibronic states of mixed character:

$$P^{1/2}|36^137^1\rangle + (1\text{-}P)^{1/2}|\text{bgd}^m\rangle \xrightarrow{k_{rad}} \text{S–He} \tag{2}$$

$$\xrightarrow{k_{vp}} S(0^0) + He.$$

While the radiative rates from the 36^137^1 and background states should be identical, the vibrational predissociation rates may be many orders of magnitude different[29] and may depend sensitively on the exact nature of the coupled background states. In the most extreme case $k_{vp} \ll k_{rad}$ for a state with high 36^137^1 character while $k_{vp} \gg k_{rad}$ for a predominantly background character state. In this limit all the resonance fluorescence would be from the 36^137^1-like state while all the dissociated intensity would be from the van der Waals dominated state. The direct lifetime measurements of SBZ confirm that $k_{vp} \gg k_{rad}$ for those states that lead to predissociation ($k_{vp}/k_{rad} = 80$). On the other hand, the lack of broadened emission in our dispersed fluorescence spectrum and the presence of narrow resonance fluorescence peaks suggests that $k_{vp} \ll k_{rad}$ for the predominantly 36^137^1 character states. As a result, the resonance fluorescence/0^0 product intensity ratio is reflecting the average 36^137^1/bgd state mixing of the laser-accessed states rather than the actual magnitude of the vibrational predissociation rate constant. Our observed intensity ratio would thus best be interpreted as due to accessing states with the laser which on average are roughly 20%$|36^137^1>$ and 80%$|\text{bgd}^m>$.

Similar arguments can remove an apparent inconsistency of the 37_0^2–He dispersed fluorescence spectrum with direct lifetime measurements. Recall that in this case the only observed channels were the predissociation channels to 37^1 and 0^0 levels of the stilbene product. The direct lifetime measurements show a 37^1 product rise time of less than 10 ps while the 0^0 rise time is about 45 ps. In the scheme of reactions (3a) and (3b):

$$S(37^2)\text{–}He \rightarrow S(37^1) + He \tag{3a}$$

$$\rightarrow S(0^0) + He \tag{3b}$$

we would have predicted a $\phi(37^1) \geqslant 0.82$ and equal rise times for both products. Our measurements of the actual product state distribution, on the other hand, yield $\phi(37^1) = 0.36$. Furthermore, SBZ's lifetime measurements for the two product channels differed significantly. Thus, we must once again picture predissociation as arising from a group of mixed states we prepare with the laser, each of which has the form:

$$p^{1/2}|37^2\rangle + (1-P)^{1/2}|\text{bgd}^m\rangle \rightarrow S(37^1) + He \tag{4a}$$

$$\rightarrow S(0^0) + He \tag{4b}$$

Energy gap considerations should favor $S(37^1)$ formation over $S(0^0)$ formation for the $|37^2>$ state. To quantify this, we can estimate the vibrational predissociation lifetimes associated with processes 6(a) and 6(b) using the formula of Ewing[29]:

$$\tau^{-1} = 10^{13} \exp[-\pi(\Delta n_T + \Delta n_r + \Delta n_V)] \tag{5}$$

where Δn_T,Δn_R, and Δn_V are the changes in translation, rotation, and vibrational quantum numbers between initial and final states in the predissociation process. Using a stilbene–He van der Waals stretching frequency equal to that of tetrazine–He(38 cm^{-1}) and an upper state binding energy equal to our upper limit estimate of 47 cm^{-1}, we obtain a $\tau(37^1)$ of 5 ps (ignoring rotational effects). A vibrational predissociation rate this fast is almost without precedent and reflects the very small change in both translational and vibrational quantum numbers[29] during the predissociation process from this level. On the other hand, the 0^0 rise time expected from the 37^2 level is calculated to be about a factor of 400 times slower than this(i.e., $\tau = 2$ ns). Thus, from $P^{1/2}|37^2>$ the 37^1 channel will dominate. In contrast, pre-

dissociation from the $|bgd^m>$ states will likely be statistically spread between the available product channels. Since translational states will dominate the density of product channels, the largest density of product channels will be from those built on the lowest stilbene vibronic level, the 0^0 level. Thus, we feel confident in associating 37^1 formation with 37^2 character [reaction 4(a)] in the stilbene–He complex and 0^0 product formation with bgd^m character [reaction 4(b)]. Since at the top of the 37_0^2 transition, $\phi(37^1) = 0.36$, we would estimate that the states accessed by the laser at the peak of the major 37_0^2 stilbene–He transition are, on average, actually only $36\%|37^2>$ and $64\%|bgd^m>$. *Thus, as with the $36^1 37^1$ level, the product state distribution we observe from this level is for the most part simply reflecting the degree of intramolecular–intermolecular mixing of the state and provides little information on the absolute magnitudes of the vibrational predissociation rate constants.* We thus see that direct lifetime measurements and product state distributions determined from the dispersed fluorescence spectrum provide complementary information on the stilbene–He complex. In this regard, it would be very interesting to see how the lifetimes of the 37^1 and 0^0 product channels would depend on where one excited in the broadened contour. It would also be interesting to know how big a role the rotational state character plays in the predissociation rates and product state distributions.

Product state distributions from higher-lying out-of-plane stilbene–He levels further confirm the generalizations just made. The 37_0^4–He and $36_0^1 37_0^3$–He levels have dispersed fluorescence spectra which are dominated by emission from the 0^0 level of the dissociated stilbene product. In particular, the 37_0^4–He dispersed fluorescence spectrum shows only two major product state levels, 0^0 and 37^3 with the 0^0 level having roughly twice the population of the 37^3 level. This 0^0-dominated distribution occurs despite the fact that there are many other levels energetically open to the stilbene products. Once again, the group of states accessed by the laser are each in actuality a mixture both intramolecular (i.e., 37^4) and intermolecular (i.e., bgd^m) in character. As with the $36^1 37^1$ and 37^2 levels, the observed product state distribution to first order simply reflects the percentages of intramolecular and intermolecular character in the laser-formed initial states. The 37^4 character will favor the lowest energy gap channel, 37^3. The background states, if they are coupled to the product state channels in a statistical fashion, will favor high translational energy products built on the lowest intramolecular level. Thus, vibrational predissociation and intramolecular–intermolecular state mixing cannot be viewed as separate phenomena in these systems but are closely tied to one another.

By contrast, the in-plane vibrational levels (e.g., 25^1 and 25^2) show little, if any, 0^0 products. Instead, they are dominated by emission from a new, unassigned stilbene vibronic level which is likely of either b_g or b_u character. The observed ratio of resonance fluorescence to dissociated product emission yields a lifetime estimate of about 200 ps, quite close to that observed experimentally from direct lifetime measurements (156 ps).[19] Thus, the levels accessed by the laser for these in-plane vibrations of the stilbene–He complex exhibit a much smaller percentage of van der Waals state character than their out-of-plane counterparts. This is not to say that coupling to the van der Waals modes is completely absent from these levels. The broadened dispersed fluorescence spectra from the 25_0^1 level of stilbene–H_2 suggests otherwise. However, while in-plane motions show only moderate coupling to the in-plane van der Waals modes, the out-of-plane motions are extremely strongly coupled to these motions. These results are in keeping with Ewing's insight[29] that is is the out-of-plane component of the intramolecular vibration in aromatic–X complexes which is the source of the coupling with the van der Waals modes. All in all, the dramatically different behavior of stilbene motions involving out-of-plane vs in-plane motions in these complexes is truly remarkable.

V. CONCLUSION

The *trans*-stilbene–X van der Waals complexes have shown themselves to be unusual subjects in several respects. We have shown that in the stilbene–He and stilbene–H_2 complexes, the He atom or H_2 molecule undergo nearly free motion between the two phenyl rings of *trans*-stilbene. These pseudotranslation states are selectively and strongly coupled to the low-energy out-of-plane phenyl ring motions of the stilbene chromophore. The low energy of both the phenyl ring and van der Waals motions have set them in relative isolation from other motions of the molecule and have thus provided a clear view of the extent and role of intramolecular–intermolecular state mixing in these complexes. In particular, the mixing of the out-of-plane phenyl ring motions with the pseudo-translation van der Waals bending modes plays a dominant role in both the unusual appearance of the fluorescence excitation spectrum and in vibrational predissociation from stilbene levels involving out-of-plane phenyl ring motion. It will be interesting to carry out similar measurements on other large molecule van der Waals complexes in order to determine the generality of the large, mode-selective state mixing we observed here.

ACKNOWLEDGMENTS

The authors gratefully acknowledge the support of the National Science Foundation (CHE-8710016) for this research. T.S.Z. also wishes to thank Calvin College for a Calvin Faculty Research Fellowship which provided a reduced teaching load during the time the research was carried out.

[1] F. G. Celii and K. C. Janda, Chem. Rev. **86**, 507 (1986).
[2] R. E. Miller, J. Phys. Chem. **90**, 3301 (1986).
[3] D. C. Dayton and R. E. Miller, Chem. Phys. Lett. **143**, 181 (1988).
[4] K. W. Jucks and R. E. Miller, J. Chem. Phys. **86**, 6637 (1987).
[5] Z. S. Huang, K. W. Jucks, and R. E. Miller, J. Chem. Phys. **85**, 3338 (1986).
[6] R. E. Miller (to be published).
[7] D. F. Coler, R. E. Miller, and R. O. Watts, J. Chem. Phys. **82**, 3555 (1985).
[8] K. G. Baldwin and R. O. Watts, Chem. Phys. Lett. **129**, 237 (1986).
[9] G. Fischer, R. E. Miller, P. F. Vohralik, and R. O. Watts, J. Chem. Phys. **83**, 1471 (1985).
[10] W. R. Gentry, in *NATO Advanced Workshop on Structure and Dynamics of Weakly Bound Molecular Complexes*, edited by A. Weber (Reidel, Dordrecht, 1987); A. Mitchel, M. J. McAliffe, C. F. Giese, and W. R.

Gentry, J. Chem. Phys. **83**, 4271 (1985).
[11]K. W. Butz, D. L. Catlett, G. E. Ewing, D. Krajnovich, and C. S. Parmenter, J. Phys. Chem. **90**, 3533 (1986).
[12]H-K. O, C. S. Parmenter, and M. C. Su, Ber. Bunsenges Phys. Chem. **92**, 253 (1988).
[13]D. V. Brumbaugh, J. E. Kenny, and D. H. Levy, J. Chem. Phys. **78**, 3415 (1983).
[14]H. Abe, Y. Okyanagi, M. Ichijo, N. Mikami, and M. Ito, J. Phys. Chem. **89**, 3512 (1985).
[15]C. A. Taatjes, W. B. Bosma, and T. S. Zwier, Chem. Phys. Lett. **128**, 127 (1986).
[16]L. H. Spangler, R. van Zee, and T. S. Zwier, J. Phys. Chem. **91**, 2782 (1987).
[17]T. Suzuki, N. Mikami, and M. Ito, J. Phys. Chem. **90**, 6432 (1986).
[18]A. Warshel, J. Chem. Phys. **62**, 214 (1975).
[19]D. H. Seemes, J. S. Baskin, and A. H. Zewail, J. Am. Chem. Soc. **109**, 4104 (1987).
[20]P. M. Felker and A. H. Zewail, J. Phys. Chem. **89**, 5402 (1985).
[21]P. M. Felker and A. H. Zewail, J. Chem. Phys. **82**, 2961 (1985).
[22]T. S. Zwier, E. Carrasquillo M., and D. H. Levy, J. Chem. Phys. **78**, 5493 (1983).
[23]G. Brocks and T. Huygen, J. Chem. Phys. **85**, 3411 (1986).
[24]D. Bahatt, U. Even, and J. Jortner, Chem. Phys. Lett. **117**, 527 (1985).
[25]J. S. Baskin, P. M. Felker, and A. H. Zewail, J. Chem. Phys. **84**, 4708 (1986).
[26]G. Herzberg, *Infrared and Raman Spectra*(Van Nostrand, New York, 1945), p. 221.
[27]S. Mukamel, J. Chem. Phys. **82**, 2867 (1985).
[28]G. A. Voth, J. Chem. Phys. **87**, 5272 (1987).
[29]G. E. Ewing. J. Phys. Chem. **91**, 4662 (1987); **90**, 1790 (1986).